Seagrass habitat metabolism increases short-term extremes and long-term offset of CO_2 under future ocean acidification

Stephen R. Pacella[a,b,1], Cheryl A. Brown[a], George G. Waldbusser[b], Rochelle G. Labiosa[c], and Burke Hales[b]

[a]Western Ecology Division, National Health and Environmental Effects Research Laboratory, Office of Research and Development, United States Environmental Protection Agency, Newport, OR 97365; [b]College of Earth, Ocean, and Atmospheric Sciences, Oregon State University, Corvallis, OR 97331; and [c]Region 10, United States Environmental Protection Agency (EPA), Seattle, WA 98101

Edited by David M. Karl, University of Hawaii, Honolulu, HI, and approved February 16, 2018 (received for review March 7, 2017)

The role of rising atmospheric CO_2 in modulating estuarine carbonate system dynamics remains poorly characterized, likely due to myriad processes driving the complex chemistry in these habitats. We reconstructed the full carbonate system of an estuarine seagrass habitat for a summer period of 2.5 months utilizing a combination of time-series observations and mechanistic modeling, and quantified the roles of aerobic metabolism, mixing, and gas exchange in the observed dynamics. The anthropogenic CO_2 burden in the habitat was estimated for the years 1765–2100 to quantify changes in observed high-frequency carbonate chemistry dynamics. The addition of anthropogenic CO_2 alters the thermodynamic buffer factors (e.g., the Revelle factor) of the carbonate system, decreasing the seagrass habitat's ability to buffer natural carbonate system fluctuations. As a result, the most harmful carbonate system indices for many estuarine organisms [minimum pH_T, minimum Ω_{arag}, and maximum $pCO_{2(s.w.)}$] change up to 1.8×, 2.3×, and 1.5× more rapidly than the medians for each parameter, respectively. In this system, the relative benefits of the seagrass habitat in locally mitigating ocean acidification increase with the higher atmospheric CO_2 levels predicted toward 2100. Presently, however, these mitigating effects are mixed due to intense diel cycling of CO_2 driven by aerobic metabolism. This study provides estimates of how high-frequency pH_T, Ω_{arag}, and $pCO_{2(s.w.)}$ dynamics are altered by rising atmospheric CO_2 in an estuarine habitat, and highlights nonlinear responses of coastal carbonate parameters to ocean acidification relevant for water quality management.

ocean acidification | seagrasses | carbonate chemistry | water quality standards | buffer factors

Ocean acidification (OA) due to increasing atmospheric CO_2 from anthropogenic emissions increases the dissolved inorganic carbon ($[TCO_2]$) and partial pressure of seawater CO_2 ($pCO_{2(s.w.)}$), and decreases seawater pH_T and carbonate mineral saturation states (e.g., Ω_{arag}). These changes in marine chemistry have been demonstrated to negatively affect acid–base balance, biocalcification, and metabolism of coastal and estuarine organisms (1). Many observational studies of OA have focused in open ocean (2) and shelf waters (3–5), with fewer studies investigating how rising atmospheric CO_2 interacts with estuarine carbonate chemistry (6, 7). The carbonate chemistry in estuarine habitats is highly variable (7, 8) due to high rates of photosynthesis and respiration, hydrodynamic processes (including tides, freshwater inputs, and estuarine circulation), biogenic calcification and dissolution, gas exchange, and strong benthic–pelagic biogeochemical coupling (9, 10). The resulting dynamic range of high-frequency estuarine carbonate chemistry calls into question the impact of rising atmospheric CO_2 levels as a driver in these systems (10, 11), with suggestions that OA (as defined above) is predominant only in open-ocean environs (12).

There is, however, an emerging appreciation for the role of high-frequency (i.e., subhourly time scales) carbonate chemistry dynamics influencing organismal responses to OA (10, 13). However, despite the significance of the coastal zone to ecosystems and our economy, our understanding of how natural and anthropogenic processes control estuarine carbonate chemistry is generally limited to studies of large spatial and/or low temporal resolution (6, 14, 15), with relatively little mechanistic examination. Thus, our understanding of how the global baseline increase in atmospheric CO_2 interacts with habitat-specific, high-frequency carbonate chemistry dynamics, or "carbonate weather," (10) to alter the chemical environment of estuarine organisms is poorly understood. The fundamental thermodynamic properties of the marine carbonate system predict that an increase in baseline $[TCO_2]$ levels will amplify the dynamic ranges of pH and $pCO_{2(s.w.)}$, and dampen that of Ω_{arag} (16). The two studies we are aware of that have investigated this response of the carbonate system [in coral reef (17) and coastal shelf (4) systems] to future OA have highlighted the importance of this altered buffering capacity of the carbonate system, resulting in larger modeled dynamic ranges of $pCO_{2(s.w.)}$ and pH_T, and reduced dynamic ranges of Ω_{arag} (4, 18). Attribution of the drivers of CO_2 dynamics responsible for the large dynamic ranges observed in estuaries permits a more rigorous and mechanistic analysis of how interactions between OA and nearshore, habitat-specific carbonate weather may be expected to accelerate carbonate conditions demonstrated to be harmful for coastal organisms (e.g., low pH, high $pCO_{2(s.w.)}$, low Ω_{arag}). This mechanistic approach to attribution of natural versus anthropogenically driven

Significance

The impacts of ocean acidification in nearshore estuarine environments remain poorly characterized, despite these areas being some of the most ecologically important habitats in the global ocean. Here, we quantify how rising atmospheric CO_2 from the years 1765 to 2100 alters high-frequency carbonate chemistry dynamics in an estuarine seagrass habitat. We find that increasing anthropogenic carbon reduces the ability of the system to buffer natural extremes in CO_2. This reduced buffering capacity leads to preferential amplification of naturally extreme low pH and high $pCO_{2(s.w.)}$ events above changes in average conditions, which outpace rates published for atmospheric and open-ocean CO_2 change. Seagrass habitat metabolism drives these short-term extreme events, yet ultimately reduces organismal exposure to harmful conditions in future high-CO_2 scenarios.

Author contributions: S.R.P., C.A.B., G.G.W., R.G.L., and B.H. designed research; S.R.P. and C.A.B. performed research; B.H. contributed new reagents/analytic tools; S.R.P., G.G.W., and B.H. analyzed data; and S.R.P. and G.G.W. wrote the paper.

The authors declare no conflict of interest.

This article is a PNAS Direct Submission.

Data deposition: This dataset has been published via the EPA Office of Research and Development Environmental Dataset Gateway (https://edg.epa.gov; doi: 10.23719/1407616).

See Commentary on page 3745.

[1]To whom correspondence should be addressed. Email: spacella@coas.oregonstate.edu.

This article contains supporting information online at www.pnas.org/lookup/suppl/doi:10.1073/pnas.1703445115/-/DCSupplemental.

Published online April 2, 2018.

carbonate dynamics is also crucial for informing pressing management decisions related to coastal water quality (19, 20).

The objectives of this study were to (*i*) characterize the carbonate weather in a shallow seagrass habitat typical of the Puget Sound estuarine system at time scales relevant to individual organisms, (*ii*) deconvolve the observed chemical time series into the primary biological and physical drivers through mechanistic modeling, and (*iii*) use these model results of present-day processes to illustrate the effect of OA on carbonate weather in the seagrass habitat under preindustrial through future emission scenario conditions. We focused on the dry season (July through September), which is a critical period of growth and recruitment for many estuarine producer and consumer species in Puget Sound (21). Our analyses focused on how the interaction of OA and aerobic metabolism in this habitat controls the onset and severity of exposure to low pH_T, high $pCO_{2(s.w.)}$, and low Ω_{arag} conditions for resident organisms currently and into the future.

Results and Discussion

High-resolution (15-min frequency) observations of pH_T from July 15–October 1, 2015, in a seagrass habitat of Hat Island in Puget Sound, WA, showed large variability on time scales consistent with local diel photosynthesis/respiration cycles, tidal advection of metabolically altered water parcels, and wind-driven mixing events (mean pH_T = 8.08, SD = 0.16, max pH_T = 8.43, min pH_T = 7.59, n = 7,455) (*SI Appendix*, Fig. S1). The mean diel range of pH_T for the period of observation was 0.39 (SD = 0.16, n = 78 d) units, with a maximum observed diel range of 0.74 units, similar to published observations from other metabolically intensive coastal systems (4, 9, 22). pH_T was significantly correlated with O_2 (R^2 = 0.91, P < 0.001; *SI Appendix*, Fig. S2), demonstrating the role of aerobic metabolism (primary production + respiration) in observed carbonate chemistry variability. Tidal exchange was documented by sampling the water masses representing mixing end members for the Hat Island site as: (*i*) marine deep water (sampled at 50 m) entering Possession Sound to the south of Hat Island, and (*ii*) the Snohomish River (23, 24). The marine end member was characterized by consistently low pH_T and elevated TCO_2 (mean = 7.66, SD = 0.02, n = 5; $[TCO_2]$ = 2,024 μmol kg^{-1}, SD = 9.2 μmol kg^{-1}; [Alk] = 2,061 μmol kg^{-1}, SD = 10.1 μmol kg^{-1}) and low O_2 (mean = 194.5 μmol kg^{-1}, SD = 9.7 μmol kg^{-1}, n = 5), consistent with published observations of deep marine waters in Puget Sound, whose ultimate source has been traced back to delivery of North Pacific Ocean waters through the Strait of Juan de Fuca via estuarine circulation (6, 25). In contrast, the Snohomish River displayed variable pH_T and lower TCO_2 (mean = 7.88, SD = 0.40, n = 5; $[TCO_2]$ = 572 μmol kg^{-1}, SD = 45 μmol kg^{-1}; [Alk] = 555 μmol kg^{-1}, SD = 27 μmol kg^{-1}) and higher O_2 (mean = 290.7 μmol kg^{-1}, SD = 9.7 μmol kg^{-1}, n = 5) compared with deep marine waters. Salinities at Hat Island (mean = 27.96, SD = 0.80, n = 7,455) indicated strong influence of marine deep waters, with a relatively small amount of freshwater dilution during the dry season.

To characterize the primary processes responsible for the observed variability of carbonate chemistry in the seagrass habitat, we developed a deterministic model (termed the "full model") that included tidal mixing (via salinity variance), net community metabolism (NCM; via O_2/CO_2 stoichiometry), and gas exchange processes (*Materials and Methods* and *SI Appendix*). The full model reproduced 92% of the observed variance in the pH_T time series (Pearson product correlation, r = 0.957; P < 0.001; Fig. 1*A*), and also showed good agreement with calculated values of $pCO_{2(s.w.)}$ and Ω_{arag} (Fig. 1 *B* and *C*) from discrete samples with measured $[TCO_2]$, $pCO_{2(s.w.)}$, and pH_T (Satlantic SeaFET) taken next to in situ sensors ($pCO_{2(s.w.)}$ root mean squared error (RMSE) = 13.5 μatm, r = 0.99, P < 0.001; Ω_{arag} RMSE = 0.19, r = 0.94, P < 0.001), and with published carbonate system values observed near our study site (26). The NCM estimates were on average responsible for 66% (SD = 26%) and 35% (SD = 31%) of modeled $[TCO_2]$ and [Alk] variability in the full model, respectively (*SI Appendix*, Fig. S3). Conservative mixing of the marine and riverine end members accounted for an average of 34% (SD = 26%) and 65% (SD = 31%) of modeled $[TCO_2]$ and [Alk] variability, respectively. Gas exchange was episodically important during the observational period, but generally a small component of the high-frequency $[TCO_2]$ variability due to low wind speeds and relatively slow exchange rates of CO_2 due to carbonate system buffering (*SI Appendix*, Fig. S3). Observations indicated the study site was within a stable surface mixed layer for the majority of the dry-season observational period; larger gas exchange fluxes from equilibration between locally upwelled high CO_2 waters and the atmosphere likely occurred earlier during the spring transition and shoaling/formation of the observed surface mixed layer (27).

We simulated the impacts of changing atmospheric CO_2 from 1765 to 2100 using the representative concentration pathway (RCP) 8.5 emissions scenario (28) both to hindcast and forecast how carbonate weather of the system is altered. These simulations estimate the state of the observed system (based on year 2015 dynamics of aerobic metabolism and mixing) under different levels of atmospheric CO_2, with the 1765 scenario representing the carbonate chemistry of the habitat if fossil fuels were never burned. Modeled anthropogenic $[TCO_2]$ (C_{anth}) in 2015 ranged from 47 to 59 μmol kg^{-1}. Estimates of C_{anth} for nearshore surface waters of the California

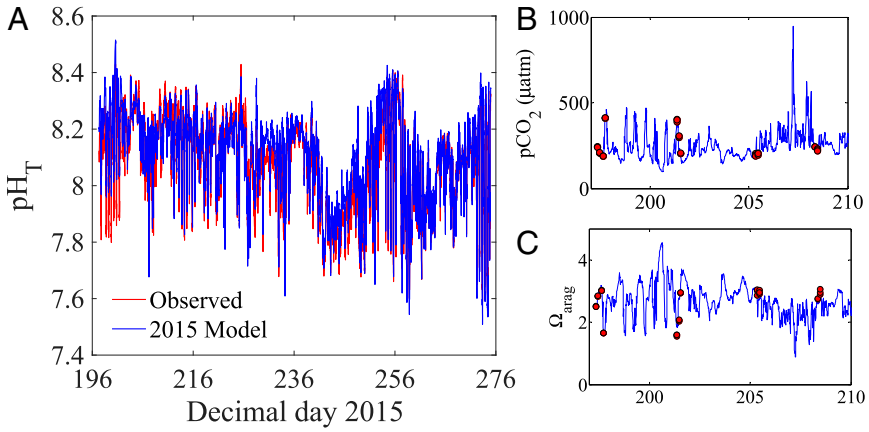

Fig. 1. (*A*) Time series (15-min frequency) of measured pH (red) at Hat Island and modeled pH (blue) of the full model. The Pearson correlation coefficient for the model was r = 0.957, P < 0.001. (*B*) Modeled pCO_2 (blue line) with calculated values (red dots) from grab samples taken at the study site. (*C*) Modeled $\Omega_{aragonite}$ (blue line) with calculated values (red dots) from grab samples taken at the study site. Calculated parameters used SeaFET pH, and measured pCO_2 and $[TCO_2]$ values for calculation of the carbonate system using CO2SYS.

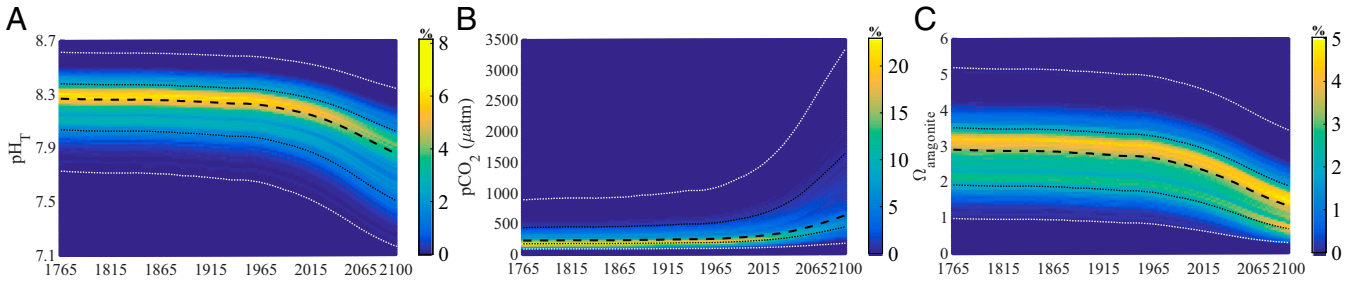

Fig. 2. Results of OA scenario models from 1765 to 2100. Color maps represent the percent occurrence for (*A*) pH_T, (*B*) $pCO_{2(s.w.)}$, and (*C*) Ω_{arag} as a function of time. Bold dashed lines represent the annual dry-season median, black dotted lines are the average daily dry-season minimum and maximum observations, and white dotted lines are annual dry-season maximum and minimum observations. Note differences between medians and modes for each parameter, indicative of the nonnormal distributions of each parameter for a given year.

Current in the year 2012 have been previously published as 52–58 μmol kg^{-1} (15) and 62 μmol kg^{-1} (4), which compare well with our mean model estimate of 53 μmol kg^{-1} for the same year. The small discrepancies among the values can be attributed to differences in temperature, salinity, and alkalinity of surface waters in the studies; warm, fresh, low alkalinity waters (such as those found at the Hat Island study site) hold relatively less C_{anth} when theoretically equilibrated with a given atmospheric CO_2 level. Results of these yearly 1765–2100 OA simulation models provide estimates of how pH_T, Ω_{arag}, and $pCO_{2(s.w.)}$ high-frequency dynamics (i.e., carbonate weather) in an estuarine habitat are altered by rising atmospheric CO_2.

Model results indicate that OA alters both means/medians and diel ranges of pH_T, $pCO_{2(sw)}$, and Ω_{arag} in the seagrass habitat, resulting in more rapid changes to extreme events relative to means/medians (Fig. 2). Median dry-season pH_T decreased 0.12 units from the preindustrial (year 1765) to 2015, with a total median reduction of 0.41 units expected by the year 2100 under the RCP 8.5 emission scenario (*SI Appendix*, Table S1), equivalent to an increase in acidity of 32% in 2015, and 157% by 2100. Compared with the year 1765, mean $pCO_{2(sw)}$ increased by 107 μatm (+45%) in 2015 and 548 μatm (+227%) in 2100, while mean dry-season Ω_{arag} decreased by 0.56 units (−20%) in 2015, and 1.50 units (−54%) in 2100. In addition to these changes in the median/mean values, changes to the thermodynamic buffer factors of the carbonate system (driven by increasing C_{anth}) altered diel ranges of pH_T, $pCO_{2(sw)}$, and Ω_{arag} (*SI Appendix*, Table S1). Previous work (16, 29) has shown that the sensitivities of pH_T, $pCO_{2(sw)}$, and Ω_{arag} (defined here as $\Delta x/\Delta[TCO_2]$, where x is the carbonate parameter of interest) respond differently to changes in $[TCO_2]$. Briefly, pH_T is most sensitive near the point where $[TCO_2] = [Alk]$, $pCO_{2(s.w.)}$ is increasingly sensitive to increasing $[TCO_2]$, and Ω_{arag} is decreasingly sensitive to increasing $[TCO_2]$. These sensitivities, delineated by the thermodynamic buffer factors of the marine carbonate system, are responsible for the behavior as illustrated in Fig. 3: diel ranges of pH_T, $pCO_{2(s.w.)}$, and Ω_{arag} of the preindustrial, 2015, and 2100 models change through time with increasing OA, despite diel ranges of $[TCO_2]$ remaining largely unchanged for all model years. The mean diel pH_T range at the study site was amplified by 0.06 units in 2015, and 0.18 units in 2100, compared with year 1765. Diel $pCO_{2(s.w.)}$ ranges were also amplified by OA, with increases of 176 μatm (+67%) and 932 μatm (+352%) in 2015 and 2100, respectively. Conversely, the mean diel range of Ω_{arag} was at its maximum in the preindustrial, having decreased by 0.08 units (−5%) in 2015 and 0.40 units (−25%) in 2100 with increasing OA (note the severity of low Ω_{arag} conditions worsens with increasing OA, however, as the absolute change outweighs the decrease in range; Fig. 2). These changes in variance of carbonate weather due to altered buffering is analogous to recently predicted (30) and observed (31) amplification of carbonate system variability on seasonal time scales in open-ocean environments.

The altered carbonate system buffering capacity due to OA causes a preferential amplification of extreme conditions, and thus a more rapid change in the most harmful OA conditions to transient life stages of organisms in these environments, such as bivalve larvae. This is due to the fact that amplification of diel ranges is asymmetrical (Fig. 4); the carbonate system becomes more sensitive to a given addition of respiratory CO_2 than an equivalent photosynthetic CO_2 removal with increasing OA. Respiration-driven extremes of low pH, high $pCO_{2(s.w.)}$, and low Ω_{arag} become preferentially worse, with larger (+105%, +17%, and +53% in 2100, respectively; *SI Appendix*, Fig. S4*A*) and more rapid (up to 1.8×, 2.3×, and 1.5×, respectively; *SI Appendix*, Fig. S4*B*) changes compared with medians/means. These changes also outpace published changes in open-ocean carbonate parameters (2), contemporary atmospheric CO_2 (28), and maximal rates of atmospheric CO_2 change during glacial–interglacial cycles in the past 800,000 y (32). Currently, indices of Ω_{arag} have progressed farthest toward their estimated 2100 values (35–52% of expected changes; *SI Appendix*, Fig. S4*C*) compared with other carbonate parameters (19–26% of expected changes), indicating organisms and habitats sensitive to Ω_{arag} are more likely to respond first to OA. The extent of this effect would depend heavily on the organism's dependence on calcification; however, laboratory studies (33) and field observations (34, 35) support

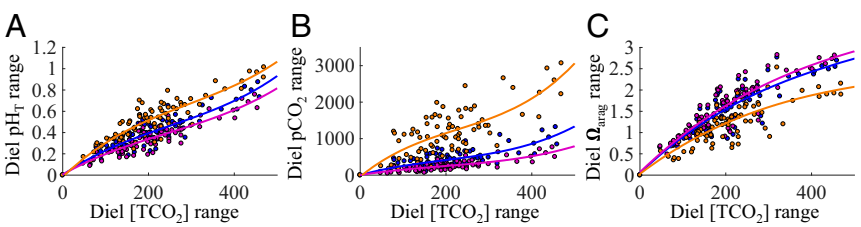

Fig. 3. Scatterplots of daily (*A*) pH, (*B*) pCO_2, and (*C*) $\Omega_{aragonite}$ ranges versus daily $[TCO_2]$ ranges for the preindustrial (1765, purple), present-day (2015, blue), and 2100 (orange) model scenarios. Each point represents a single day (July 15–October 1) in the model (n = 78). Lines are third-degree polynomial lines of best fit for each of the model scenarios.

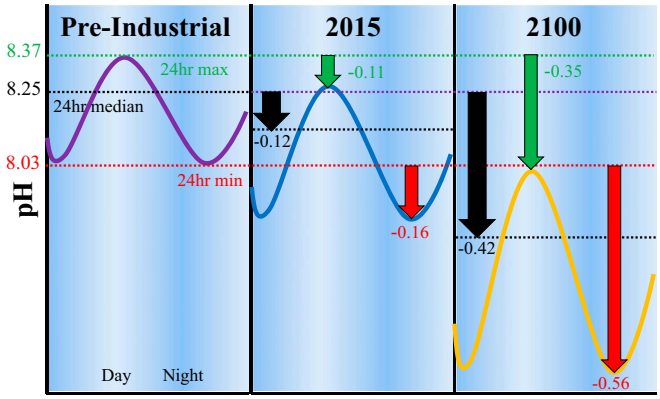

Fig. 4. Representative diel curves illustrating changes in daily pH medians (black), maximums (green), and minimums (red) from preindustrial values for years 2015 and 2100. Daily pH minimums have larger reductions than corresponding medians and maximums due to the additive anthropogenic and respiratory carbon reducing the pH buffering capacity of the system. Values shown are mean changes for the dry season of the designated year.

the concept of present-day calcification-related OA stress for organisms as well as ecosystems (36, 37).

A potential OA mitigation strategy that has been proposed for shellfish and coastal environments is the preservation and restoration of submerged aquatic vegetation (38). Although our modeling technique does not attribute the observed NCM signal to its subcomponents (e.g., seagrass vs. water column metabolism) because of the significant methodological hurdles associated with appropriate field observations (39), it does provide an opportunity to explore how integrated habitat-level metabolism alters the carbonate weather experienced by resident organisms of the seagrass habitat. The OA simulations suggest NCM in this seagrass habitat currently improves average conditions for all carbonate system variables, but drives transient extremes of low pH, high $pCO_{2(s.w.)}$, and low Ω_{arag}. NCM during the productive dry season in our study system is estimated to raise present-day (2015) dry-season median pH_T by 0.08 units, raise median Ω_{arag} by 0.33 units, and lower median $pCO_{2(s.w.)}$ by 70 μatm (Fig. 5). These effects of seagrass habitat metabolism will become increasingly important under worsening OA from an organismal OA-refugia perspective with respect to pH_T and $pCO_{2(s.w.)}$, but diminish with respect to Ω_{arag} (Fig. 5*B*). NCM will be increasingly effective at raising median pH_T (+0.07 units in 1765, +0.11 units in 2100) and reducing median $pCO_{2(s.w.)}$ (−44 μatm in 1765, −199 μatm in 2100), but less effective at raising median Ω_{arag} (+0.35 units in 1765, +0.28 units in 2100) with increasing atmospheric CO_2 levels. Although NCM improves average conditions in this habitat, NCM is also responsible for driving the natural extremes of the habitat's carbonate weather; minimum dry-season pH is reduced by 0.49 units, minimum dry-season Ω_{arag} is reduced by 1.15 units, and maximum dry-season $pCO_{2(s.w.)}$ is raised by 1,033 μatm in 2015 (Fig. 5*B*). As discussed, these NCM-driven extremes of low pH_T and high $pCO_{2(s.w.)}$ are amplified with increasing atmospheric CO_2 levels. Conversely, decreased sensitivity of Ω_{arag} at higher $[TCO_2]$ levels causes the addition of anthropogenic carbon to slightly reduce the relative importance of NCM in driving minimum Ω_{arag} levels.

The decoupling of carbonate system averages and extremes illustrates a dichotomous role of NCM in metabolically vigorous environments facing rising atmospheric CO_2: increasing the severity of transient poor carbonate chemistry in the present and near-future, and ultimately reducing organismal exposure to harmful carbonate conditions in a future, high CO_2 world. For example, our model predicts seagrass habitat NCM effectively delays median dry-season Ω_{arag} from crossing an established larval shellfish calcification threshold (Ω_{arag} = 1.4) by 26 y; equivalent to buffering against a 215-ppmv increase in atmospheric CO_2. However, low Ω_{arag} periods driven by NCM cause average dry-season daily minimums of Ω_{arag} to cross this same threshold 44 y earlier than estimated in the absence of NCM. This concept is illustrated in Fig. 6, where we compare exceedance of previously published harmful and exceptionally favorable Ω_{arag} thresholds for larval bivalves (33) due to increasing OA in the presence and absence of NCM. Presently, NCM increases the duration of time during which Ω_{arag} conditions for bio-calcification are exceptionally favorable ($\Omega_{arag} > 2.8$) by 37%, while also causing the exceedance of demonstrated harmful thresholds for calcification ($\Omega_{arag} < 1.4$) that would not be experienced for another 43 y in the absence of aerobic metabolism. However, an inflection point in time is reached in the future (year 2061, atmospheric CO_2 = 611 ppmv), at which point NCM reduces the duration of negative threshold exceedance compared with the models run without NCM. This is due to the large diel ranges of carbonate parameters driven by NCM, resulting in windows of favorable carbonate conditions associated with short-term photosynthetic reductions of $[TCO_2]$. Tolerance thresholds for carbonate parameters have been experimentally shown to be species specific (40); therefore, the timing of these inflection points will differ among species, but the general pattern illustrated in Fig. 6 can still be expected.

Conceptually, metabolically intensive coastal zones may ameliorate the negative effects of OA on organisms via temporal

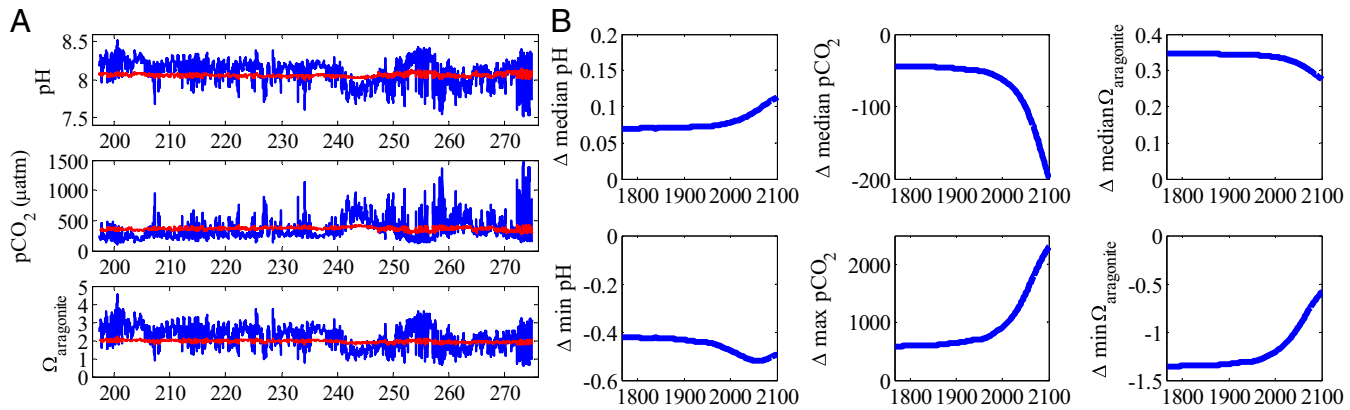

Fig. 5. Comparison of OA simulation models with (full) and without (abiotic) the net community metabolism term. *A* shows a comparison of model output for the full model (blue) and the abiotic model (red) of model year 2015 (July 15–October 1). *B* illustrates the differences in median and extremes of carbonate parameters between the full and abiotic models from 1765 to 2100. The *y*-axis deltas are equal to the full model parameter minus the abiotic model parameter. For example, NCM elevates median dry-season pH by ~0.07 units in 1765, but decreases minimum dry-season pH by ~0.42 units.

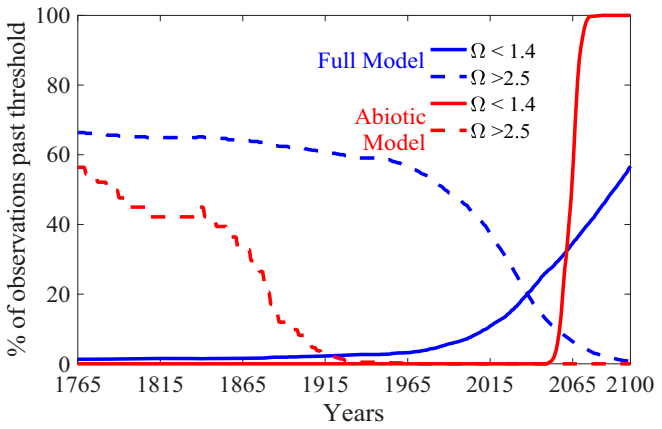

Fig. 6. Percentage of observations for each OA model simulation year exceeding published harmful (solid lines) and exceptionally favorable (dashed lines) thresholds of $\Omega_{aragonite}$ for biocalcification of larval bivalves. Compared is output from all model simulations for the full (with NCM; blue lines) and abiotic (without NCM; red lines) models. The $\Omega_{aragonite}$ thresholds from refs. 1 and 33. Conditions were similarly favorable for biocalcification in the preindustrial with or without NCM's influence on carbonate chemistry. Currently, NCM increased incidence of exceptionally favorable and harmful conditions. In future high-CO_2 scenarios, incidences of exceptionally favorable conditions are nearly absent, regardless of NCM; however, NCM greatly reduces the incidence of harmful conditions.

windows of favorable pH_T and $pCO_{2(s.w.)}$ (e.g., productive daytime hours) despite decreasing baselines, or conversely exacerbate these negative effects via the enhanced magnitudes and exposure durations of low pH_T and high $pCO_{2(s.w.)}$. Although researchers are beginning to explore how short-term carbonate weather influences organismal responses to OA (41, 42), most OA experiments have focused on measuring effects due to static exposure of organisms following long experimental acclimation periods. These methodologies fail to capture the realistic carbonate weather of many nearshore habitats. The ability to cope with changing variances of carbonate chemistry will likely be an important determinant of acclimation and ultimately genetic adaptation among taxa with increasing OA, highlighting the need for a better understanding of organismal responses to variable conditions (13, 41, 43–45). This may be most important for species with temporally short, but OA-sensitive, developmental stages, such as marine bivalve larvae (1). Our model predicts Ω_{arag} has already reached a mean daily minimum value below established harmful thresholds [$\Omega_{arag} < 1.4$ (33, 46)] for early calcification of some bivalve larvae in 2013. Organisms often live close to tolerance thresholds in estuarine habitats (10), and so although adaptation to naturally variable environments can enhance resilience to stress (47), exceedance of these tolerance thresholds by increasingly frequent and more extreme events (as demonstrated in this study) can still be expected (48).

The decoupling of the averages and extremes of carbonate parameters with increasing anthropogenic CO_2 (Figs. 2 and 4 and *SI Appendix*, Fig. S4) also poses an important question for OA-related water quality standards: what really matters? Our study has shown that the carbonate parameters previously identified as being most stressful for coastal organisms [minimum pH_T and Ω, maximum $pCO_{2(s.w.)}$] are changing more rapidly than their corresponding averages—the index frequently used in water quality standards. The US Environmental Protection Agency recommended criteria for most marine waters states that pH should not be changed more than 0.2 units outside of the naturally occurring range and should not be outside the range of 6.5–8.5 units; Washington State includes this provision in their water quality standards (49). If we assume carbonate system variability in the 1765 model represents this naturally occurring range, the minimum dry-season pH_T has already exceeded this Δ0.2 unit threshold in 2012, and median pH_T is not expected to exceed a Δ0.2 unit threshold until 2045. Existing standards are, therefore, likely insufficient to account for carbonate weather-scale impacts on coastal ecosystems—the very scale experienced by resident organisms. Although there are currently no recommended water quality standards for other carbonate parameters, analogous issues exist for $pCO_{2(s.w.)}$ and Ω_{arag}. Additionally, environmental management resulting in nutrient reductions could be expected to help offset some OA effects on water quality (19), but may also lower baseline pH_T levels [and raise $pCO_{2(s.w.)}$] of estuarine habitats due to reduced net ecosystem production in surface waters. Further study is necessary to understand the impact of anthropogenic nutrients in controlling carbonate chemistry dynamics in shallow, nearshore environments. Efficacy of OA-related management decisions will depend on matching time and space scales of interventions with those of system-specific drivers of carbonate chemistry, and the specific exposure duration, magnitude, and frequency of exceedance of the OA parameter(s) of interest to the most sensitive organisms.

Our analyses indicate that as anthropogenic CO_2 continues to increase in the atmosphere, the carbonate system in this seagrass habitat becomes less able to buffer natural sources of high-frequency CO_2 variance, causing nonlinear amplification of naturally extreme events. Increasing OA will result in similar patterns of amplified changes in the variability and extremes of other metabolically vigorous estuarine and marine systems due to altered buffering with increasing anthropogenic carbon (16, 29). This predicted amplification of carbonate system variability is beginning to emerge in open-ocean observations on seasonal time scales (31), supporting the underlying mechanisms of more extreme carbonate weather in estuaries with OA. The magnitude of change in carbonate weather due to this altered buffering capacity will be a function of the initial "natural" carbonate buffer factors of the system, as well as the intensity of high-frequency carbon cycling.

Materials and Methods

The study site was located in a shallow subtidal seagrass habitat (48° 01.20′N, 122° 19.39′W) on the northern shore of Hat (Gedney) Island, WA, in Possession Sound. The seagrass habitat consisted of a dense stand of *Zostera marina* (canopy height ~ 1 m) typical of fringing shoreline seagrass beds, which make up ~50% of all seagrass habitat in the whole of Puget Sound (50). Sensor packages were anchored to the benthos with sensing units ~30 cm above the bottom. Water depth ranged from 0.62 to 4.98 m, with a mean of 3.19 m. Time series measurements of pH_T, O_2, salinity, temperature, and depth were collected every 15 min during the study period using YSI 6000 series sondes. Sondes were replaced with a calibrated sonde every ~4 wk, and checked for fouling and drift after deployments. A Satlantic SeaFET sensor was deployed from July 1 to July 15 to verify accuracy of the YSI pH measurements (*SI Appendix*, Fig. S5). Sensors were factory calibrated, and verified with Certified Reference Material CO_2 standards from the University of California, San Diego (Batch 132). Grab samples for sensor validation were stored in sealed 330-mL amber glass bottles using established protocols for dissolved gas sampling, and analyzed for $[TCO_2]$ and pCO_2 at Oregon State University. The Marine Deep end member was sampled at 50 m depth at the southern end of Possession Sound near Mukilteo (47° 58.05′N, 122° 18.08′W). The Snohomish River end member was sampled at river mile 10.6 (47° 56.25′N, 122° 10.14′W). Carbonate chemistry of the end members was calculated with CO_2SYS [Matlab version 1.1; K1 and K2 constants of Millero (51); KSO_4 constants of Dickson (52); borate:salinity of Lee et al. (53)] using paired in situ YSI pH_{NBS} and $[TCO_2]$, or paired $[TCO_2]$ and $pCO_{2(s.w.)}$ (when available) from grab samples.

To reconstruct the observed pH time series at Hat Island, changes from initial measured $[TCO_2]$ and calculated [Alk] (using $[TCO_2]$ and SeaFET pH_T) on July 1 were estimated using a model that incorporated mixing of the marine and riverine end members, aerobic photosynthesis and respiration (i.e., net community metabolism), and gas exchange of O_2 and CO_2 (*SI Appendix*). Mixing ratios of riverine and marine end member $[TCO_2]$ and [Alk] were determined using observed salinities at Hat Island. The dissolved oxygen time series was corrected for gas exchange and mixing of riverine and marine end members, and used to estimate aerobic metabolism using a metabolic quotient (ΔO_2:ΔTCO_2) of 1.05 [following published values for seagrass habitats (54)]. Concurrent metabolic alterations of [Alk] were estimated using the Redfield ratio of 16:117 for ΔAlk:ΔTCO_2. A $CaCO_3$ calcification/dissolution term was not

included due to insufficient data to constrain these processes on the time scales of the model. High correlation between model output and observations suggest these processes are not dominant drivers of carbonate weather in this system during the modeled time period. The modeled values of [TCO_2] and [Alk] for each time point were used to compute the full carbonate system using CO_2SYS (Matlab version 1.1) (Dataset S1), and results were corrected for gas exchange of CO_2 to produce the full model final results using 2015 as a base year.

$$[TCO_2]_{t+1} = [TCO_2]_t + \Delta[TCO_2]_{\text{mixing}} + \Delta[TCO_2]_{\text{metabolism}} + \Delta[TCO_2]_{\text{gas}}$$

$$[Alk]_{t+1} = [Alk]_t + \Delta[Alk]_{\text{mixing}} + \frac{16}{117}\Delta[TCO_2]_{\text{metabolism}}$$

To isolate and quantify the effect of aerobic metabolism on carbonate weather in the seagrass habitat, we ran the model with (full model) and without (abiotic model) the metabolic term in the model. This procedure was repeated for all OA scenario models for the years 1765–2100.

Historic and future carbonate weather was estimated using two methods for calculating anthropogenic CO_2: an adaptation of the ΔC^* method (assuming constant air–sea disequilibrium with respect to [TCO_2]; ref. 55), and an adaptation of the ΔpCO_2 method (6, 7) (assuming constant air–sea disequilibrium with respect to pCO_2; *SI Appendix*). We report the results of the $\Delta[TCO_2]$ method here for clarity, and include the results of the adapted ΔpCO_2 method in the *SI Appendix*. The $\Delta[TCO_2]$ method produces the more conservative results, with both methods supporting the conclusions of this manuscript (see *SI Appendix* for discussion).

ACKNOWLEDGMENTS. We thank the Tulalip Tribes, T. Chris Mochon Collura, and Dr. Jim Kaldy for assistance with field work, and Dr. Lauren Juranek and two reviewers for improving this manuscript. This project was funded by a US EPA Regional Applied Research Effort Program grant.

1. Waldbusser GG, et al. (2015) Ocean acidification has multiple modes of action on bivalve larvae. *PLoS One* 10:e0128376.
2. Bates NR, et al. (2012) Detecting anthropogenic carbon dioxide uptake and ocean acidification in the North Atlantic Ocean. *Biogeosciences* 9:2509–2522.
3. Feely RA, Sabine CL, Hernandez-Ayon JM, Ianson D, Hales B (2008) Evidence for upwelling of corrosive 'acidified' water onto the continental shelf. *Science* 320:1490–1492.
4. Takeshita Y, et al. (2015) Including high-frequency variability in coastal ocean acidification projections. *Biogeosciences* 12:5853–5870.
5. Sutton AJ, et al. (2016) Using present-day observations to detect when anthropogenic change forces surface ocean carbonate chemistry outside pre-industrial bounds. *Biogeosci Discuss* 13:5065–5083.
6. Feely RA, et al. (2010) The combined effects of ocean acidification, mixing, and respiration on pH and carbonate saturation in an urbanized estuary. *Estuar Coast Shelf Sci* 88:442–449.
7. Hales B, Suhrbier A, Waldbusser GG, Feely RA, Newton JA (2016) The carbonate chemistry of the 'fattening line,' Willapa Bay, 2011–2014. *Estuaries Coast* 40:173–186.
8. Hinga KR (1992) Co-occurrence of dinoflagellate blooms and high pH in marine enclosures. *Mar Ecol Prog Ser* 86:181–187.
9. Hofmann GE, et al. (2011) High-frequency dynamics of ocean pH: A multi-ecosystem comparison. *PLoS One* 6:e28983.
10. Waldbusser GG, Salisbury JE (2014) Ocean acidification in the coastal zone from an organism's perspective: Multiple system parameters, frequency domains, and habitats. *Annu Rev Mar Sci* 6:221–247.
11. Wallace RB, Baumann H, Grear JS, Aller RC, Gobler CJ (2014) Coastal ocean acidification: The other eutrophication problem. *Estuar Coast Shelf Sci* 148:1–13.
12. Duarte CM, et al. (2013) Is ocean acidification an open-ocean syndrome? Understanding anthropogenic impacts on seawater pH. *Estuaries Coast* 36:221–236.
13. Small DP, et al. (2016) Temporal fluctuations in seawater pCO_2 may be as important as mean differences when determining physiological sensitivity in natural systems. *ICES J Mar Sci* 73:604–612.
14. Provoost P, van Heuven S, Soetaert K, Laane RWPM, Middelburg JJ (2010) Seasonal and long-term changes in pH in the Dutch coastal zone. *Biogeosciences* 7:3869–3878.
15. Feely RA, et al. (2016) Chemical and biological impacts of ocean acidification along the west coast of North America. *Estuar Coast Shelf Sci* 183:260–270.
16. Egleston ES, Sabine CL, Morel FMM (2010) Revelle revisited: Buffer factors that quantify the response of ocean chemistry to changes in DIC and alkalinity. *Global Biogeochem Cycles* 24:1–9.
17. Shaw EC, McNeil BI, Tilbrook B, Matear R, Bates ML (2013) Anthropogenic changes to seawater buffer capacity combined with natural reef metabolism induce extreme future coral reef CO_2 conditions. *Glob Change Biol* 19:1632–1641.
18. Shaw EC, McNeil BI, Tilbrook B (2012) Impacts of ocean acidification in naturally variable coral reef flat ecosystems. *J Geophys Res Oceans* 117:C03038.
19. Kelly MW, Padilla-Gamiño JL, Hofmann GE (2013) Natural variation and the capacity to adapt to ocean acidification in the keystone sea urchin *Strongylocentrotus purpuratus*. *Glob Change Biol* 19:2536–2546.
20. Strong AL, Kroeker KJ, Teneva LT, Mease LA, Kelly RP (2014) Ocean acidification 2.0: Managing our changing coastal ocean chemistry. *Bioscience* 64:581–592.
21. Miller JJ, Maher M, Bohaboy E, Friedman CS, McElhany P (2016) Exposure to low pH reduces survival and delays development in early life stages of Dungeness crab (*Cancer magister*). *Mar Biol* 163:1–11.
22. Baumann H, Wallace RB, Tagliaferri T, Gobler CJ (2014) Large natural pH, CO_2 and O_2 fluctuations in a temperate tidal salt marsh on diel, seasonal, and interannual time scales. *Estuaries Coast* 38:220–231.
23. Yang Z, Wang T, Voisin N, Copping A (2015) Estuarine response to river flow and sea-level rise under future climate change and human development. *Estuar Coast Shelf Sci* 156:19–30.
24. Banas NS, et al. (2015) Patterns of river influence and connectivity among subbasins of Puget Sound, with application to bacterial and nutrient loading. *Estuaries Coast* 38:735–753.
25. Murray JW, et al. (2015) An inland sea high nitrate-low chlorophyll (HNLC) region with naturally high pCO_2. *Limnol Oceanogr* 60:957–966.
26. Pelletier G, Roberts M, Keyzers M, Alin SR (2018) Seasonal variation in aragonite saturation in surface waters of Puget Sound–A pilot study. *Elem Sci Anth* 6:5.
27. Moore-Maley BL, Allen SE, Ianson D (2016) Locally driven interannual variability of near-surface pH and ΩA in the Strait of Georgia. *J Geophys Res Oceans* 121:1600–1625.
28. Riahi K, et al. (2011) RCP 8.5-A scenario of comparatively high greenhouse gas emissions. *Clim Change* 109:33–57.
29. Hagens M, Middelburg JJ (2016) Generalised expressions for the response of pH to changes in ocean chemistry. *Geochim Cosmochim Acta* 187:334–349.
30. Kwiatkowski L, Orr JC (2018) Diverging seasonal extremes for ocean acidification during the twenty-first century. *Nat Clim Chang* 8:141–146.
31. Landschützer P, Gruber N, Bakker DCE, Stemmler I, Six KD (2018) Strengthening seasonal marine CO_2 variations due to increasing atmospheric CO_2. *Nat Clim Chang* 8:146–150.
32. Lüthi D, et al. (2008) High-resolution carbon dioxide concentration record 650,000-800,000 years before present. *Nature* 453:379–382.
33. Waldbusser GG, et al. (2015) Saturation-state sensitivity of marine bivalve larvae to ocean acidification. *Nat Clim Chang* 5:273–280.
34. Bednaršek N, et al. (2014) *Limacina helicina* shell dissolution as an indicator of declining habitat suitability owing to ocean acidification in the California Current Ecosystem. *Proc Biol Sci* 281:20140123.
35. Barton A, Hales B, Waldbusser GG, Langdon C, Feely RA (2012) The Pacific oyster, *Crassostrea gigas*, shows negative correlation to naturally elevated carbon dioxide levels: Implications for near-term ocean acidification effects. *Limnol Oceanogr* 57:698–710.
36. Dove SG, et al. (2013) Future reef decalcification under a business-as-usual CO_2 emission scenario. *Proc Natl Acad Sci USA* 110:15342–15347.
37. Albright R, et al. (2016) Reversal of ocean acidification enhances net coral reef calcification. *Nature* 531:362–365.
38. Washington State Blue Ribbon Panel on Ocean Acidification (2012) *Ocean Acidification: From Knowledge to Action, Washington State's Strategic Response*, eds Adelsman H, Whitely Binder L (Washington Department of Ecology, Olympia, Washington), Publication no. 12-01-015.
39. Long MH, Berg P, Falter JL (2015) Seagrass metabolism across a productivity gradient using the eddy covariance, Eulerian control volume, and biomass addition techniques. *J Geophys Res Oceans* 120:3624–3639.
40. Gazeau F, et al. (2013) Impacts of ocean acidification on marine shelled molluscs. *Mar Biol* 160:2207–2245.
41. Shaw EC, Munday PL, McNeil BI (2013) The role of CO_2 variability and exposure time for biological impacts of ocean acidification. *Geophys Res Lett* 40:4685–4688.
42. Hofmann GE, Todgham AE (2010) Living in the now: Physiological mechanisms to tolerate a rapidly changing environment. *Annu Rev Physiol* 72:127–145.
43. Reum JCP, et al. (2014) Interpretation and design of ocean acidification experiments in upwelling systems in the context of carboante chemsitry co-variation with temperature and oxygen. *ICES J Mar Sci* 71:528–536.
44. Li F, Wu Y, Hutchins DA, Fu F, Gao K (2016) Physiological responses of coastal and oceanic diatoms to diurnal fluctuations in seawater carbonate chemistry under two CO_2 concentrations. *Biogeosci Discuss* 13:6247–6259.
45. Clark H, Gobler C (2016) Do diurnal fluctuations in CO2 and dissolved oxygen concentrations provide a refuge from hypoxia and acidification for early life stage bivalves? *Mar Ecol Prog Ser* 558:1–14.
46. Ekstrom JA, et al. (2015) Vulnerability and adaptation of US shellfisheries to ocean acidification. *Nat Clim Chang* 5:207–214.
47. Schoepf V, Stat M, Falter JL, McCulloch MT (2015) Limits to the thermal tolerance of corals adapted to a highly fluctuating, naturally extreme temperature environment. *Sci Rep* 5:17639.
48. Hauri C, Gruber N, McDonnell AMP, Vogt M (2013) The intensity, duration, and severity of low aragonite saturation state events on the California continental shelf. *Geophys Res Lett* 40:3424–3428.
49. United States Environmental Protection Agency (1986) *Quality Criteria for Water, 1986* (United States Environmental Protection Agency, Washington, DC), EPA Publication no. 440/5-86-001.
50. Christiaen B, Ferrier L, Dowty P, Gaeckle J, Berry H (2017) *Puget Sound Seagrass Monitoring Report: Monitoring Year 2015* (Washington State Department of Natural Resources, Olympia, WA).
51. Millero FJ (2010) Carbonate constants for estuarine waters. *Mar Freshwater Res* 61:139–142.
52. Dickson AG (1990) Standard potential of the reaction: AgCl(s) + $12H_2$ (g) = Ag(s) + HCl (aq), and the standard acidity constant of the ion HSO_4^- in synthetic sea water from 273.15 to 318.15 K. *J Chem Thermodyn* 22:113–127.
53. Lee K, et al. (2010) The universal ratio of boron to chlorinity for the North Pacific and North Atlantic oceans. *Geochim Cosmochim Acta* 74:1801–1811.
54. Duarte CM, et al. (2010) Seagrass community metabolism: Assessing the carbon sink capacity of seagrass meadows. *Global Biogeochem Cycles* 24:1–8.
55. Matsumoto K, Gruber N (2005) How accurate is the estimation of anthropogenic carbon in the ocean? An evaluation of the ΔC^* method. *Global Biogeochem Cycles* 19:1–17.